International Information and Engineering Technology Association
Advancing the World of Information and Engineering

Ingénierie des Systèmes d'Information
Vol. 31, No. 7, July, 2026, pp. 2501-2509
Journal homepage: http://iieta.org/journals/isi

# HSI-SpaClassNet: A Deep Learning Framework for Non-Destructive Detection and Concentration Classification of Chlorpyrifos Residues on Spinach Leaves Using Hyperspectral Imaging

Sweta G. Phegade*, Monali Y. Khachane

Dr. Annasaheb. G. D. Bendale, Mahila Mahavidyalaya, Jalgaon 425001, India

Corresponding Author Email: shwetafegade@imr.ac.in



https://doi.org/10.18280/isi.310730

**Received:** 14 November 2025
**Revised:** 30 April 2026
**Accepted:** 14 May 2026
**Available online:** 31 July 2026

***Keywords:***
*hyperspectral imaging, hyperspectral imaging-spaclassnet, deep learning, Chlorpyrifos residue detection, spatial–spectral feature learning, non-destructive food safety monitoring, pesticide classification*

**ABSTRACT**

Pesticide residue contamination in agricultural products poses a significant challenge to food safety monitoring. It creates an urgent need for rapid, accurate, and non-destructive detection technologies. This study proposes hyperspectral imaging HSI-SpaClassNet, a deep learning framework that integrates HSI and deeper feature learning. The architecture is designed for detection and classification of Chlorpyrifos residues on spinach leaves. A hyperspectral dataset, namely SpinachHsiDB, was constructed using spinach samples treated with different Chlorpyrifos concentrations, including Pure, Low, Medium, and High residue levels. The proposed framework automatically extracts discriminative deeper characteristics from hyperspectral images through a customized EfficientNetB3 model. In addition, traditional machine learning (ML) classifiers and the VGG16 model were implemented for comparative evaluation. Experimental results demonstrated that HSI-SpaClassNet achieved superior classification performance. The overall accuracy achieved by the proposed architecture was 94.92%, precision of 94.95%, recall of 94.91%, and F1-score of 94.90%. Compared with conventional ML approaches, the proposed architecture showed enhanced capability in learning complex hyperspectral patterns and improving residue classification accuracy. Furthermore, Gradient-weighted Class Activation Mapping (Grad-CAM) visualization revealed the critical regions contributing to model predictions, improving the interpretability of the detection process. The proposed approach provides an efficient and reliable solution for non-destructive pesticide residue assessment and has promising potential for intelligent food safety monitoring applications.

## 1. INTRODUCTION

Spinach (*Spinacia oleracea* L.) is a well-known vegetable with high nutritional value. It is rich in all the essential minerals, such as calcium and iron, and a variety of bioactive compounds like carotenoids, vitamin C, and vitamin K. It also contains coenzyme Q10 and other nutrients that are beneficial, making it an important ingredient of a diet and promoting health [1]. Pesticides are natural or artificial compounds that are used to manage pests, weeds, and diseases in plants in agricultural systems. The examples are herbicides, insecticides, fungicides, rodenticides, and nematicides. These chemicals are central to crop safeguarding and boosting farm output [2]. Image processing is also essential in the area of machine learning (ML), especially in the machine detection and recognition of objects, as in agricultural detection and recognition settings. The research paper aims at identifying pesticide residues on spinach by means of hyperspectral imaging (HSI) and ML algorithms. HSI is a fast-growing area in digital imaging applications that offers a high spectral resolution, enabling to make accurate material classification per pixel. This technology combines machine vision with spectroscopy by obtaining spectral and spatial data. Thus simultaneously allows the analysis of the internal and external characteristics of a sample in one processing chain [3]. HSI uses the term hyper to refer to the large number of measured wavelength bands, which are a feature of very large datasets. The technique uses spectroscopy to obtain hundreds of images, creating a rich pool of data related to the object under study. The inspection of the pixel is performed with the light of illuminated sensors, which in turn are separated into numerous different spectral bands [4]. The use of algorithms in hyperspectral image processing is related to capturing, storing, and updating data. It helps in analysis, classification, regression, target identification, and pattern recognition. These steps are also important in providing facilities in data mining and making informed decisions and conditions in a variety of applications [5].

The development of HSI has become visible in the last few decades because of its ability to analyze agricultural products in a nondestructive manner. The technology allows the overall measurement of internal and external quality parameters of fruit and vegetable samples without damage to the integrity of the specimens. There are various applications of ML, such as K-Nearest Neighbor (KNN), Support Vector Machine (SVM), Decision Tree (DT), Random Forest (RF), Artificial Neural

Network (ANN) [6, 7], Convolutional Neural Network (CNN), and others. They have demonstrated successful implementation in this field to enhance detection and classification results.

The current paper begins with a systematic review of the previous studies that adopted image-processing and machine-learning algorithms on hyperspectral data. This achieves the goal of detecting pesticide contamination. Available literature is mainly related to the extraction of texture and spectral descriptors. Later, spinach leaves were imaged in the hyperspectral format with the help of a dedicated hyperspectral camera system. Single-band image slices were cut out of each spectral cube. Gray-Level Co-occurrence Matrix (GLCM) properties were retrieved to form a structured feature matrix. Several supervised learning algorithms, including SVM, KNN, RF, and ANN, were applied to the resulting dataset. A deep learning architecture, the VGG16 model and HSI-SpaClassNet, extracted the spatial and low-level spectral (intensity features) based on the band image. The extracted features were then used to train and test the model.

Accuracy, F1-score, precision, and recall were used to determine model performance. The results mentioned in the fourth section were used to provide a comparative study of the traditional machine-learning technique, deep learning techniques, and the suggested HSI-SpaClassNet framework. This shows that the multiple deep features result in an appreciable increase in classification ability. The conclusion, final part, summarises the study's key findings and offers some form of recognition.

## 2. LITERATURE SURVEY

The current study assessed various chemical, physical, and computational methodologies used in the detection of pesticide residues in agricultural products. Literature synthesis provided valuable insights about the methods used to detect non-destructive residues on surfaces. The literature in the field that documents their remaining work employs a wide range of methods. Starting with image-processing and hyperspectral analysis to machine-learning and deep learning that are discussed in a variety of matrices of fruits and vegetables.

Several studies have demonstrated the potential of machine-learning algorithms in the classification of residue. An example is that Ren et al. [4] achieved an accuracy of 99.7 percent on dimethoate on spinach leaves by using Linear Discriminant Analysis (LDA). Xiang et al. [5] used the Con1dResNet architecture to forecast the firmness and soluble solid content of cherry tomatoes, and achieved the best performance. Hu et al. [8] used Visible and Near-Infrared (VNIR) and Short-Wave Infrared (SWIR) HSI with a One-Dimensional Convolutional Neural Network (1D-CNN) to achieve 94.00 percent accuracy to detect pesticides on Hami-melon. Hu et al. [9] further elaborated on work using the Honey Badger Algorithm with an adaptive t-distribution mutation strategy- Extreme Learning Machine (tHBA-ELM) models to achieve 93.50 percent pesticide detection rates on Hami melons. Sun et al. [10] used a CNN on lettuce with pesticides with 88 percent accuracy. Fernández-Rosales et al. [11] used a Multilayer Perceptron (MLP) model on hyperspectral tomato data with 90 percent accuracy. Likewise, Jiang et al. [12] established that an AlexNet model used on apple images can achieve 95.35 percent accuracy. Zhu et al. [13] took advantage of HSI with the help of an ELM model to assess spinach freshness, which had a 100 percent accuracy. Jia et al.[14] classified pesticides in apple using using spectral selection and optimization methods with 95% accuracy. Sun et al. [15] applied the Competitive Adaptive Reweighted Sampling – Iteratively Retained Informative Variables – Genetic Simulated Annealing (CARS-IRIV-GSA-SVM) for lettuce samples with 98.33% accuracy. Lara et al. [16] examined the shelf-life of spinach using Visible–Near Infrared (400–1000 nm) hyperspectral imaging through transparent packaging films.

Despite these advances, Table 1 shows existing works rely on conventional ML algorithms [17, 18] or basic CNNs that require manual feature extraction, limiting their ability to capture rich information. Deep learning models used so far were not sufficiently optimized for hyperspectral data, and feature learning was often shallow or underexplored. Therefore, there is a need for a specialized deep learning model capable of effectively extracting deeper features for higher accuracy and better generalization. The research addresses this gap by introducing the HSI-SpaClassNet model, designed for enhanced feature extraction and classification of pesticide residues on spinach leaves.

**Table 1.** Summary of related studies on hyperspectral and machine learning (ML) approaches for pesticide detection

| References | Crop / Sample | Technique | Spectral Range or Data Type | Accuracy |
|---|---|---|---|---|
| Ren et al. [4] | Spinach | LDA, KNN, RF, SVC | HSI | 99.7% (LDA best) |
| Xiang et al. [5] | Cherry Tomato | Con1dResNet | VNIR HSI | Improved firmness prediction |
| Ye et al. [6] | Grapes | LR, SVM, RF, CNN, ResNet | Vis-NIR, NIR | 93–97% (SVM/LR best) |
| Phegade et al. [7] | Spinach | KNN, SVM, RF | HSI | RF: 86.39% |
| Hu et al. [8] | Hami Melon | 1D-CNN with attention | VNIR & SWIR HSI | 94.0% |
| Hu et al. [9] | Hami Melon | THBA-ELM | SWIR HSI | 93.5% |
| Sun et al. [10] | Lettuce | CNN | RGB / HSI | 88% |
| Fernández-Rosales et al. [11] | Tomato | MLP (Neural Network) | Hyperspectral Camera | 90% |
| Jiang et al. [12] | Apple | AlexNet (CNN) | RGB / HSI | 95.35% |
| Zhu et al. [13] | Spinach | ELM | HSI | 100% |
| Jia et al. [14] | Apple | LDA, SVM, KNN, DT, Ensemble | Spectral features | 95% (Ensemble best) |
| Sun et al. [15] | Lettuce | CARS-IRIV-GSA-SVM | NIR spectroscopy | 98.33% |
| Lara et al. [16] | Spinach | Visible–Near Infrared | Hyperspectral reflectance image | Monitoring freshness and aging of spinach leaves during storage |

| | | | | |
|---|---|---|---|---|
| Cong et al. [19] | Lettuce | GSA-SVM | NIR Spectroscopy | 96.08% |
| Mohite et al. [20] | Grapes | PCA, LASSO, ElasticNet + SVM, RF, ANN | RGB features | 91.98% (SVM best) |
| Tsuta et al. [21] | Spinach | SVM vs. LDA | Hyperspectral excitation–emission | SVM > LDA |
| Jiang et al. [22] | Black vegetable | MCEWM | HSI | 94.20% |
| He et al. [23] | Chinese cabbage | PLS-DA, SVM, ANNs, and principal component ANNs | NIRS | Review paper |
| Chen et al. [24] | Fruits | MC-CNN-GRU model | Raman spectroscopy curve | Reaching 99% |
| Basha et al.[25] | Okra | 3D-SERSNET | HSI | 98.07% |
| Jiang et al. [26] | Banana Peel | Deep forest (DF) algorithm | HSI | 93.28% |

Note: LDA = Linear Discriminant Analysis, KNN = K-Nearest Neighbor, RF = Random Forest, SVM = Support Vector Machine, CNN = Convolutional Neural Network, DT = Decision Tree, ANN = Artificial Neural Network, HSI = Hyperspectral imaging, SVC = Support Vector Classification, PCA = Principal Component Analysis.

## 3. METHODOLOGY

### 3.1 Sample collection

A local farm business in Jalgaon district in Maharashtra, India, was selected as the source of fresh leaves of *Spinacia oleracea* L in this study. Sampling was carried out during the winter season (September to November) or early spring windows (February-March), which is a favourable phenological time for spinach growth. The rain water then used to prepare formulations of pesticides that contained Chlorpyrifos, a commonly used insecticide. The dilution of Chlorpyrifos in rainwater was developed to form three different concentrations: 1:100 (high), 1:500 (medium), and 1:1000 (low). Untreated leaves were used as control specimens. The solutions that had been formulated were sprayed evenly on the sides of the spinach leaves using a handheld atomizer. The atomizer maintained the same distance to ensure that all parts were covered evenly. After application, the leaves were air-dried and then placed in controlled indoor conditions and left to dry out for 15–16 hours before imaging.

Table 2 presents the data on the hyperspectral image camera setup and different calibration parameters that are used in the preparation of the SpinachHsiDB dataset [27].

**Table 2.** Image acquisition camera settings summary

| Parameter | Specification |
|---|---|
| Imaging system | Resonon Pika hyperspectral imaging (HSI) spectroradiometer |
| Spectral range | 400–1000 nm |
| Spectral bands | 300 discrete bands |
| Spectral resolution | Approximately 2.7 nm |
| Sensor position | Mounted on a stationary stand |
| Sensor elevation | 50–100 cm above sample surface |
| Lens focal length | 50 mm |
| Field of view | Approximately 10–12 cm |
| Illumination source | 150 W Quartz Tungsten Halogen (QTH) lamps |
| Lamp placement | Positioned at a 45° angle on both sides of the camera |
| Lighting condition | Uniform illumination |
| White reference | Spectralon calibration panel |
| Dark reference | Closed-lens dark frame |
| Calibration purpose | Acquisition of calibrated reflectance images |

Note: Resonon Hyperspectral Imaging Solutions Product Catalog, Nov. 2023.

### 3.2 Image acquisition

The calibration is achieved using the equation [4]:

$$R_C = \frac{R_r - R_d}{R_w - R_d} \tag{1}$$

The variables in this study are $R_r$, $R_w$, $R_d$, and $R_c$, which represent the raw, white reference, dark reference, and corrected spectral value, respectively. Scanning of the individual leaves was done, and the resultant hyperspectral data cubes were saved in ENVI format, including spatial dimensions along the x (width), y (height), and z (depth) axes. The applied setup ensured consistent imaging parameters, minimized the effect of outside radiation, and provided reproducible data that could be further processed in a later analysis [4].

### 3.3 Dataset preparation

The current study assembled a new database named SpinachHsiDB [27]. The hyperspectral pictures obtained through the camera are represented as a data cube in 3 dimensions, i.e., $f(x, y, i)$ where $x$ and $y$ are the spatial coordinates of individual pixels, and $i$ is an index of spectral bands, which has an equidistant wavelength band of 400-1000 nm, hence giving 300 spectral bands [28]. This process can be mathematically expressed as:

$$P(x, y) = f(x, y, i), \quad i \text{ is } 1,2, \dots\dots\dots.., 300 \tag{2}$$

where, $P(x, y)$ represents the intensity of the corresponding pixel in the output image, and $f(x, y, i)$ denotes the reflectance value at spatial position $(x, y)$ for the *i*-th spectral band.

The hyperspectral data cube in Figure 1 was further split into separate images in order to use it in this study. Rather than combining all useful information into a single RGB image, each wavelength band was individually preserved as a separate grayscale .png file. Each file maintained the unique reflectance characteristics associated with each spectral region. These band-wise images were then used to extract features using deep learning.

The labelling process was done on the basis of pesticide concentration ranges, decided during sample preparation. Each image was verified before labeling for the four-class assignment. High concentration images were labelled as H1_1.png, Medium concentration as M1_1.png, Low concentration as L1_1.png, and pure P1_1.png. Similarly, the remaining image labeling was done in the dataset. Data cleaning was conducted on samples, such as checking image format, dimensions, and labelling to improve dataset reliability. Figure 2 illustrates the dataset of images representing various classes of pesticide concentrations: Pure, Low, Medium, and High. The sample includes 12,000 images of spinach leaves, spread across four different classes, namely Pure, Low, Medium, and High, corresponding to the concentration of the pesticide Chlorpyrifos, respectively. The different categories consist of approximately 3,000 images, and this gives a balanced corpus that can be used in classification experiments. Table 3 illustrates the distribution of the samples by their classes in the dataset.

### 3.4 Proposed system architecture

The general map of the working scheme of the suggested model to identify pesticide concentration with the help of HSI is shown in Figure 3. The stages involved include acquisition of datasets using an authorized hyperspectral camera that records images of spinach leaves at various spectral bands. The data is preprocessed by separating band images from the HSI cube, which is shown in Figure 2. This process increases the number of images and stored in *.png format. The images provide useful information about different bands for each sample.

**Table 3.** Number of images

| Class | No. of Images | No. Training Images (80%) | No. Testing Images (20%) |
|---|---|---|---|
| Pure | 3000 | 2400 | 600 |
| Low | 3000 | 2400 | 600 |
| Medium | 3000 | 2400 | 600 |
| High | 3000 | 2400 | 600 |

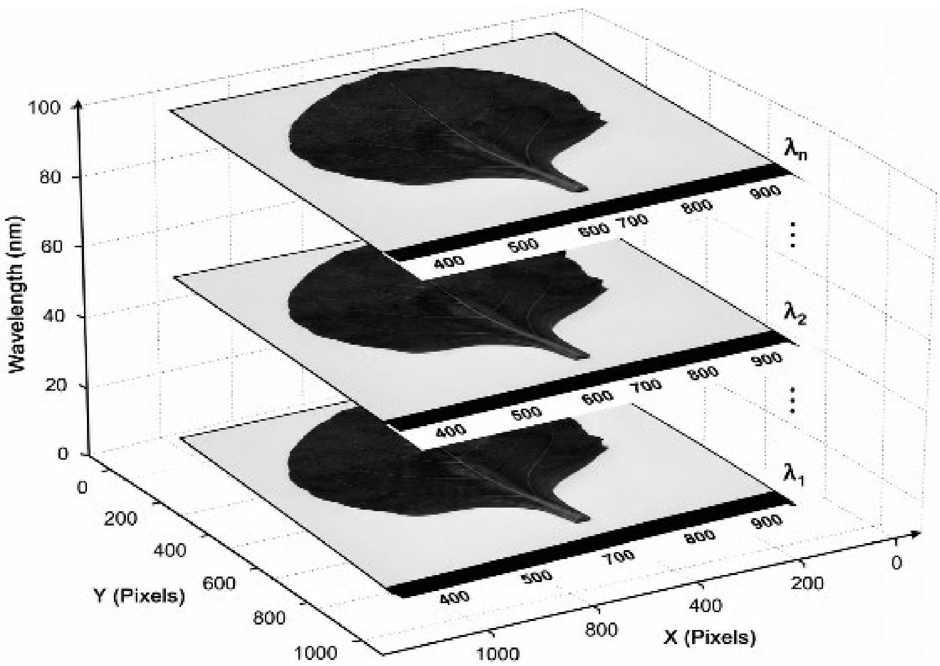


**Figure 1.** Hyperspectral image cube

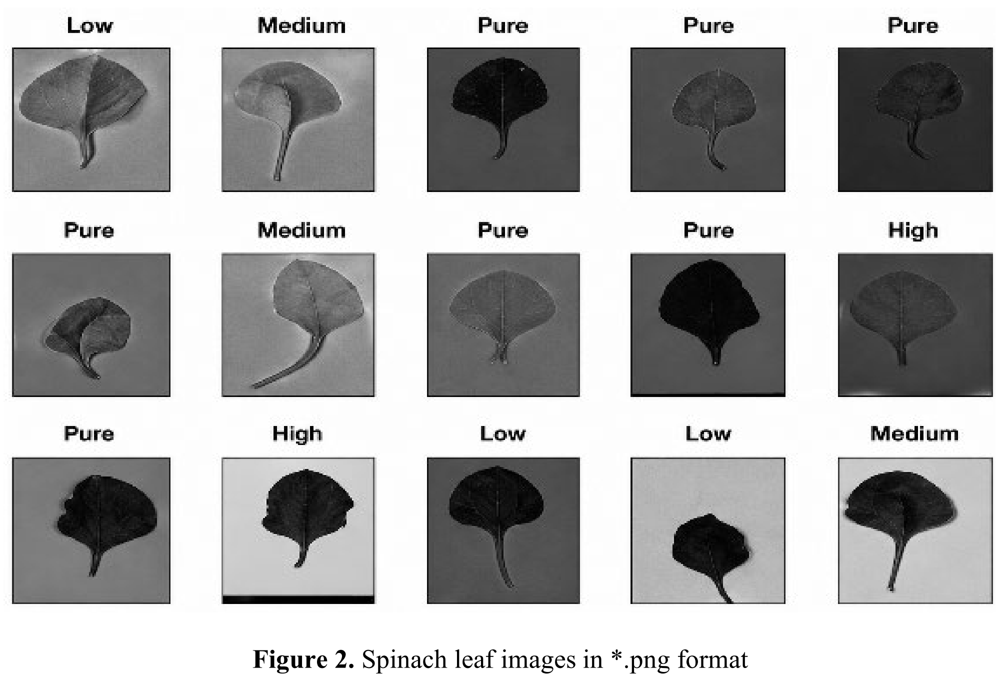


**Figure 2.** Spinach leaf images in *.png format

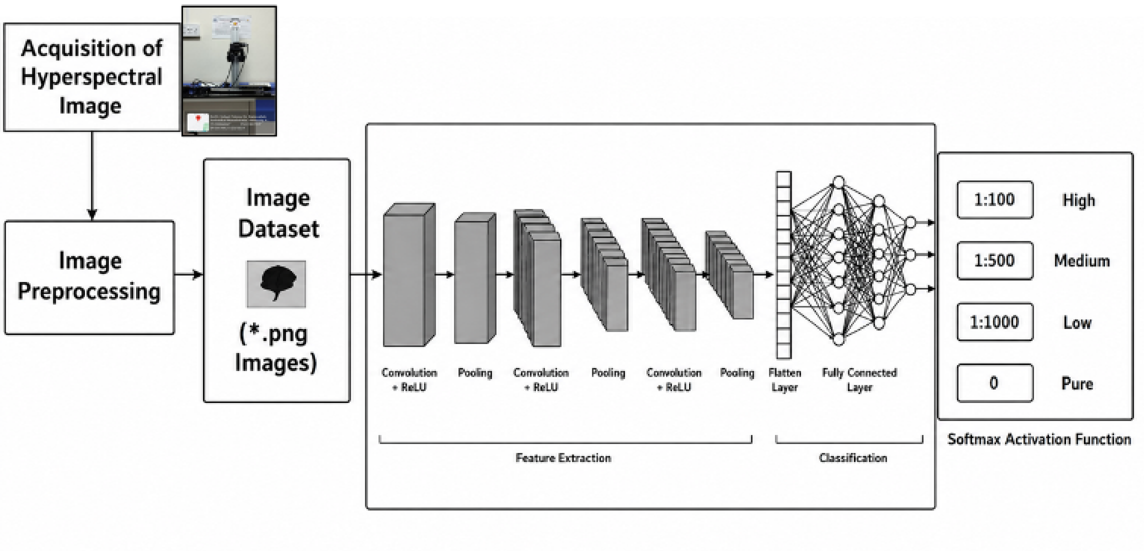


**Figure 3.** Workflow of the proposed model

GLCM values of contrast, correlation, energy, and homogeneity were derived from every band image to describe the textural properties. The feature sets produced an inclusive data set that incorporated a spatial aspect, which was used for the mentioned ML algorithms for classification. The proposed architecture, HSI-SpaClassNet, was then fed with the training image samples of different pesticide concentration levels on images. A customized EfficientNetB3 model [29, 30] was used as a feature extractor, with its base layers kept frozen. The model was tested on a testing subset after the training phase to determine its predictive accuracy. The trained model then performed automatic classification of hyperspectral images into four categories in terms of pesticide concentration levels, which are High, Medium, Low, and Pure.

To increase model interpretability, Gradient-weighted Class Activation Mapping (Grad-CAM) visualization was applied to analyze the discriminative regions learned by the proposed HSI-SpaClassNet architecture. Mathematically shown as [31],

$$L^{c}_{Grad-CAM} = ReLU(\Sigma_k \alpha^{c}_{k} A^{k}) \tag{3}$$

where,

$A^k$: Feature map,

$\alpha^c_k$: Importance weights,

$ReLU$ keeps only positive influence regions.

Grad-CAM generates a class-wise heatmap from the last convolution layer of the CNN model. It uses a gradient to find the feature map and highlights the regions of the input image that result from the model's prediction [32].

The proposed model, as shown in Algorithm 1, is a profound feature learning model that is expected to categorize the quantity of chemicals in pesticide concentrations on spinach leaves through imaging hyperspectra. The architecture enhances the separability of classes and their detection accuracy.

The proposed HSI-SpaClassNet model effectively learned deeper features. The convolutional backbone extracted low-level feature representations, while the custom classification head learned discriminative concentration-specific patterns. The key hyperparameters and training settings for the proposed architecture are listed in Table 4. These are different from traditional model parameters. This is done to achieve higher accuracy than traditional models.

**Algorithm 1.** HSI-SpaClassNet Model

Input: Hyperspectral spinach leaf images
Output: Classification into High, Medium, Low, and Pure classes

1. Start
2. Load hyperspectral image dataset.
3. Perform image preprocessing and normalization.
4. Extract deep features using the customized EfficientNetB3 model - base layers kept frozen.
5. Apply batch normalization to stabilize feature learning.
6. Pass features through a fully connected dense layer with ReLU activation.
7. Apply regularization techniques to reduce overfitting.
8. Apply dropout for improved generalization.
9. Generate class probabilities using the Softmax layer.
10. Classify images into High, Medium, Low, and Pure categories.
11. Train the network using categorical cross-entropy loss and Adamax optimizer.
12. Evaluate classification accuracy on testing data.
13. Stop.

**Table 4.** Proposed model training settings

| Hyper Parameter | Specifications |
|---|---|
| Input shape | img_shape |
| Pooling method | Max Pooling |
| Train-test data split | 80:20 |
| Epoches | 5 |
| Batch normalization momentum | 0.99 |
| Batch normalization epsilon | 0.001 |
| Dense layer units | 256 |
| Activation function | ReLU |
| L2 regularization | 0.016 |
| L1 activity regularization | 0.006 |
| Bias regularization | 0.006 |
| Dropout rate | 0.45 |
| Dropout seed | 123 |
| Output activation | Softmax |
| Optimizer | Adamax |
| Learning rate | 0.001 |
| Loss function | Categorical Crossentropy |
| Evaluation metric | Accuracy |

This combined learning mechanism enabled the model to distinguish subtle structural and spectral variations more effectively than conventional ML algorithms relying on handcrafted features alone.

## 4. RESULTS AND DISCUSSION

This model was implemented and executed on Python 3.10.9, Jupyter Notebook in VS Code on a personal computer with an i5 processor and 12 GB RAM. Figure 4 shows the training accuracy and loss curves of the proposed architecture.

The proposed model showed significant improvement over traditional ML methods and the VGG16 model, with an overall accuracy of 94.92%, a precision value of 94.95, a recall value of 94.91, and an F1-score of 94.90. The confusion matrix provided in Figure 5 shows that the model was able to isolate most of the samples; hence, validating its strong predictive power. From the confusion matrix analysis, most of the samples in the dataset were correctly classified in High and Low classes, as they showed major changes in features. However, some misclassifications were observed between Medium to High, Pure and Low classes. Most of the Medium concentration samples were misclassified as High because hyperspectral values in certain wavelength bands demonstrated similar intensity distributions. Medium class samples were misclassified into Low or Pure classes due to similarity in texture patterns or spatial characteristics between different levels. Pure class showed much better classification accuracy, as untreated spinach leaves maintained the same signatures and homogeneous surface textures. In contrast, Low and Medium concentration samples showed partial overlap due to gradual changes in chlorophyll absorption and water content effects after pesticide application. For example, from the dataset, the medium class, M9_156.png image was classified as a High class. Similarly, Low samples were classified into Medium or Pure classes for the same reason. For instance, from the dataset, the low class, L5_23.png image was misclassified into Pure because of a very small amount of change happened by pesticide concentration on spatial features. This finding states that the proposed deep learning architecture majorly shows effective extraction of texture, patterns, and visual characteristics that belong to different classes. Figure 6 shows the class-wise accuracies for Pure, Medium, Low, and High.

Table 5 indicates the relative performance of ML and deep learning classifiers used to classify spinach leaves under four concentration levels of pesticides, namely, High, Medium, Low, and Pure. The most reliable findings were provided by the RF model, which reached an accuracy of 87.04% and balanced values of precision, recall, and F1-score of about 87%. ANN obtained a percentage of 78.12, which corresponds to medium ability to predict non-linear relations, inherent to hyperspectral data. The KNN algorithm obtained an accuracy of 72.71%, which is low; however, its performance was affected by high-dimensional features. On the other hand, the SVM produced the lowest accuracy of 62.72 which could be due to the difficulty of defining overlapping classes involving complex hyperspectral data. The VGG16 model gives 84.45% accuracy compared to a 2D deep neural network with the proposed neural network.

Standard deviation is used to evaluate the consistency and reliability of the proposed model performance across multiple runs with different dataset splits. Five dataset splits were evaluated. The 70:30 and 75:25 splits achieved an accuracy of 94.63%, while the 80:20 split achieved an accuracy of 94.92%. The 85:15 and 90:10 splits achieved an accuracy of 95.21%, as training samples increased. The proposed model gave an accuracy of $94.92 \pm 0.29$, a precision of $94.95 \pm 0.41$, a recall value of $94.91 \pm 0.38$, and an F1-score of $94.90 \pm 0.36$. So, standard deviation values indicate that the model gives consistent performance across repeated runs.

As shown in Figure 7, the graphical comparison of classifiers clearly highlights the superiority of the proposed model. The results indicate that models capable of learning hierarchical features perform significantly better than those relying solely on hand-crafted features. Comparing this work with the literature review, this research demonstrates better performance by providing reliable accuracy on the testing set. The use of deep feature extraction enables the model to produce a meaningful representation of the data, and this leads to more accurate classification results with all four classes. Overall, the findings confirm that the proposed model provides a robust, accurate, and non-destructive approach for detecting pesticide residues on spinach leaves using HSI, making it a promising tool for practical agricultural monitoring and food safety assessment.

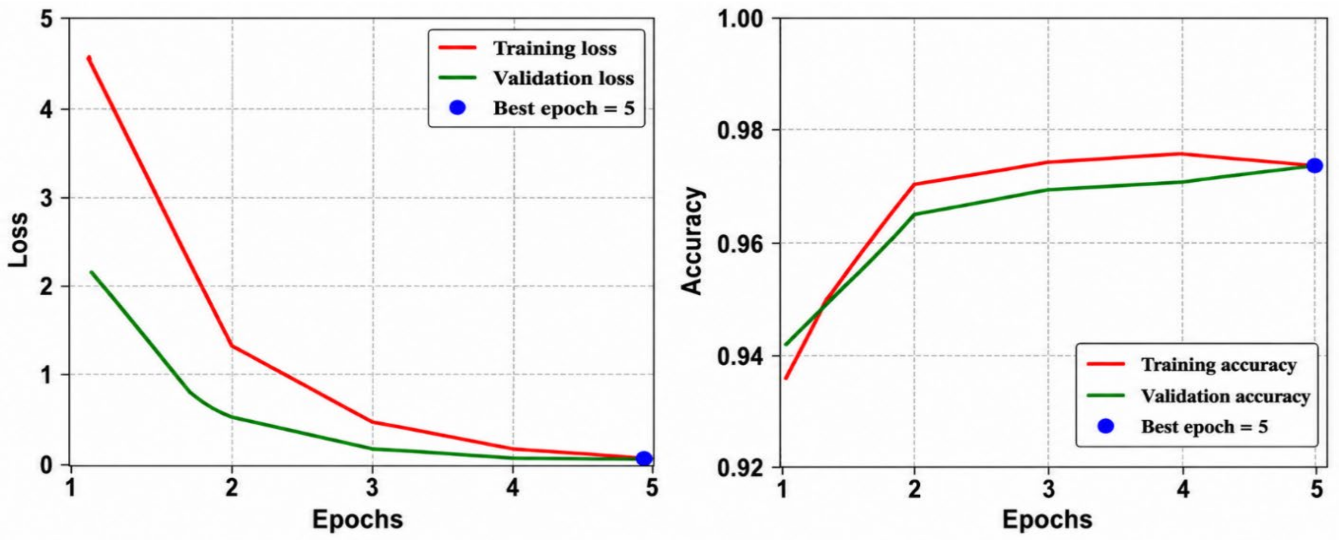


**Figure 4.** Training accuracy and loss of the proposed model

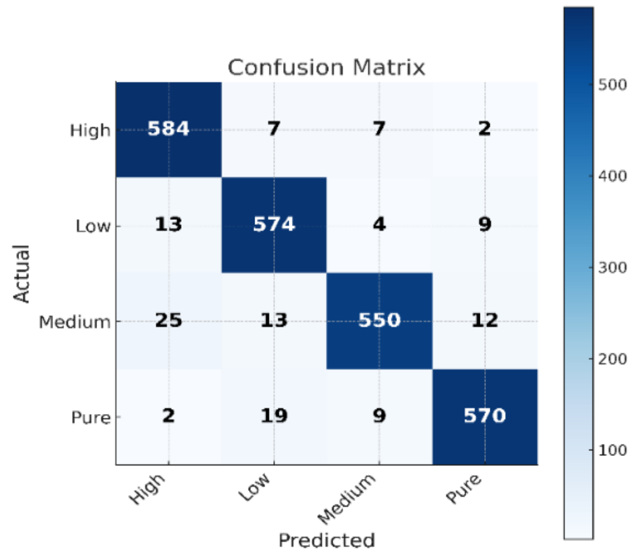


**Figure 5.** Confusion matrix of the proposed model

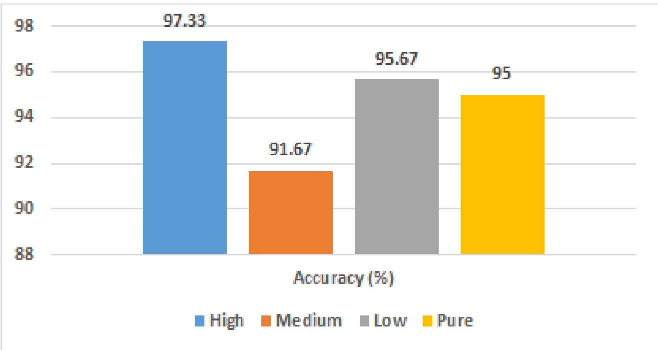


**Figure 6.** Classwise accuracy chart for the proposed model

**Table 5.** Results comparison of classifiers

| Classifier | Precision | Recall | F1-Score | Accuracy |
|---|---|---|---|---|
| KNN | 73.26 | 72.71 | 72.54 | 72.71 |
| RF | 87.08 | 87.04 | 87.02 | 87.04 |
| SVM | 63.50 | 62.80 | 62.50 | 62.72 |
| ANN | 84.41 | 78.12 | 80.42 | 78.12 |
| VGG16 | 84.25 | 83.75 | 84.25 | 84.45 |
| HSI-SpaClassNet Proposed Architecture | 94.95 | 94.91 | 94.90 | 94.92 |

Note: KNN = K-Nearest Neighbor, RF = Random Forest, SVM = Support Vector Machine, CNN = Convolutional Neural Network, ANN = Artificial Neural Network, HSI = Hyperspectral imaging.

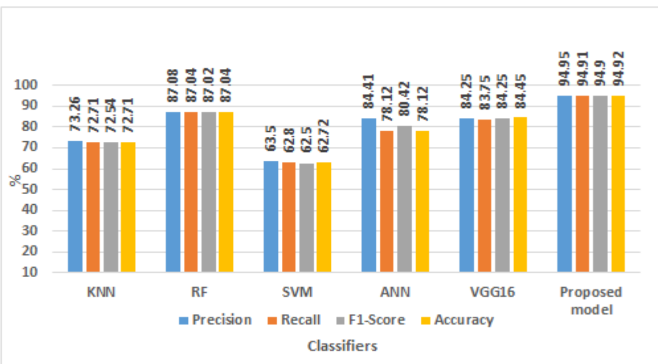


**Figure 7.** Graphical representation of performance metrics for different classifiers

## 5. CONCLUSION AND FUTURE WORK

This paper reflects a non-destructive method to identify the presence of Chlorpyrifos pesticide residues on spinach leaves with the use of the suggested HSI-SpaClassNet architecture. Hyperspectral images obtained were preprocessed and analyzed, with the achieved classification accuracy of 94.92 ± 0.29, precision of 94.95 ± 0.41, recall of 94.91 ± 0.38, and F1-score of 94.90 ± 0.36. The proposed architecture performed better as compared to traditional classifiers like SVM, RF, KNNs, and ANN. In contrast to the already existing ready-made datasets assembled in ideal laboratory settings, in this research, a self-generated SpinachHsiDB dataset was used, and it is a reflection of the real-life settings in agriculture. The results prove the capability of the HSI and deep learning in combination to detect pesticides in agricultural environments promptly, correctly, and without any destruction. Moreover, the research forms a baseline for future research to extrapolate the use of this technology to detect more contaminants and a wider range of agricultural produce. Consequently, future research should focus on different varieties of vegetables, fruits, and pesticides, as well as environmental conditions like illumination and background, to improve the accuracy of pesticide classification. In addition, advanced deep learning architectures and attention mechanisms can be used to further enhance deeper spatial–spectral feature extraction and classification accuracy. It is important to evaluate the algorithm’s reliable performance by improving statistical validations under diverse field conditions to assess its generality and robustness. IoT-based smart farming systems and portable hyperspectral devices are combined to enable rapid and non-destructive pesticide residue detection in practical applications.

## ACKNOWLEDGMENT

We would like to acknowledge the valuable assistance provided for chemical and sample preparation by Dr. Ganesh Jethve of the Chemistry Department, Dr. Annasaheb G.D. Bendale Mahila Mahavidyalaya, Jalgaon. We are also grateful to Rashtriya Uchchatar Shiksha Abhiyan (RUSA) and the Center of Advanced Sensor Technology in the Dr.Babasaheb Ambedkar Marathwada University, Chhatrapati Sambhajinagar, for offering the required instrumentation and facilities to carry out this study.

## REFERENCES

[1] Devi, P.I., Thomas, J., Raju, R.K. (2017). Pesticide consumption in India: A spatiotemporal analysis. Agricultural Economics Research Review, 30(1): 163-172. https://doi.org/10.5958/0974-0279.2017.00015.5

[2] Nayak, P., Solanki, H. (2021). Pesticides and Indian agriculture—A review. International Journal of Research Granthaalayah, 9(5): 250-263. https://doi.org/10.29121/granthaalayah.v9.i5.2021.3930

[3] Lorente, D., Aleixos, N., Gómez-Sanchis, J.U.A.N., Cubero, S., García-Navarrete, O.L., Blasco, J. (2012). Recent advances and applications of hyperspectral imaging for fruit and vegetable quality assessment. Food and Bioprocess Technology, 5(4): 1121-1142. https://doi.org/10.1007/s11947-011-0725-1

[4] Ren, Z.Q., Rao, Z.H., Ji, H.Y. (2018). Identification of different concentrations pesticide residues of dimethoate on spinach leaves by hyperspectral image technology. IFAC-PapersOnLine, 51(17): 758-763. https://doi.org/10.1016/j.ifacol.2018.08.104
[5] Xiang, Y., Chen, Q., Su, Z., et al. (2022). Deep learning and hyperspectral images based tomato soluble solids content and firmness estimation. Frontiers in Plant Science, 13: 860656. https://doi.org/10.3389/fpls.2022.860656
[6] Ye, W., Yan, T., Zhang, C., et al. (2022). Detection of pesticide residue level in grape using hyperspectral imaging with machine learning. Foods, 11(11): 1609. https://doi.org/10.3390/foods11111609
[7] Phegade, S.G., Khachane, M.Y. (2025). Non-destructive classification of pesticide residues on spinach leaves using hyperspectral imaging and machine learning algorithms. International Journal of Computer Research and Technology, 10(1): 34-38. https://basponccollege.org/ClgIJCRTJournals/IJCRT/IJCRT%20Vol-10-issue-1(i)-2025.pdf.
[8] Hu, Y., Ma, B., Wang, H., Zhang, Y., Li, Y., Yu, G. (2023). Detecting different pesticide residues on Hami melon surface using hyperspectral imaging combined with 1D-CNN and information fusion. Frontiers in Plant Science, 14: 1105601. https://doi.org/10.3389/fpls.2023.1105601
[9] Hu, Y., Ma, B., Wang, H., Li, Y., Zhang, Y., Yu, G. (2023). Non-destructive detection of different pesticide residues on the surface of Hami melon classification based on THBA-ELM algorithm and SWIR hyperspectral imaging. Foods, 12(9): 1773. https://doi.org/10.3390/foods12091773
[10] Sun, L., Cui, X., Fan, X., Suo, X., Fan, B., Zhang, X. (2023). Automatic detection of pesticide residues on the surface of lettuce leaves using images of feature wavelengths spectrum. Frontiers in Plant Science, 13: 929999. https://doi.org/10.3389/fpls.2022.929999
[11] Fernández-Rosales, C., Fernandez-Moreno, A., Álvarez-León, D., Prieto-Sánchez, S. (2022). Tomato pesticide residue detection method based on hyperspectral imaging. In 2022 17th Iberian Conference on Information Systems and Technologies (CISTI), Madrid, Spain, pp. 1-6. https://doi.org/10.23919/CISTI54924.2022.9820482
[12] Jiang, B., He, J., Yang, S., et al. (2019). Fusion of machine vision technology and AlexNet-CNNs deep learning network for the detection of postharvest apple pesticide residues. Artificial Intelligence in Agriculture, 1: 1-8. https://doi.org/10.1016/j.aiia.2019.02.001
[13] Zhu, S., Feng, L., Zhang, C., Bao, Y., He, Y. (2019). Identifying freshness of spinach leaves stored at different temperatures using hyperspectral imaging. Foods, 8(9): 356. https://doi.org/10.3390/foods8090356
[14] Jia, Y., He, J., Fu, H., Shao, X., Li, Z. (2018). Apple surface pesticide residue detection method based on hyperspectral imaging. In International Conference on Intelligent Science and Big Data Engineering, pp. 539-556. https://doi.org/10.1007/978-3-030-02698-1_47
[15] Sun, J., Ge, X., Wu, X., Dai, C., Yang, N. (2018). Identification of pesticide residues in lettuce leaves based on near infrared transmission spectroscopy. Journal of Food Process Engineering, 41(6): e12816. https://doi.org/10.1111/jfpe.12816
[16] Lara, M.A., Lleó, L., Diezma-Iglesias, B., Roger, J.M., Ruiz-Altisent, M. (2013). Monitoring spinach shelf-life with hyperspectral image through packaging films. Journal of Food Engineering, 119(2): 353-361. https://doi.org/10.1016/j.jfoodeng.2013.06.005
[17] Sarker, I.H. (2021). Machine learning: Algorithms, real-world applications and research directions. SN Computer Science, 2(3): 1-21. https://doi.org/10.1007/s42979-021-00592-x
[18] Mahesh, B. (2020). Machine learning algorithms—A review. International Journal of Science and Research, 9(1): 381-386. https://doi.org/10.21275/ART20203995
[19] Cong, S., Liu, C., Zhu, Z., Hu, A. (2021). Study on identification of multiple pesticide residues in lettuce leaves based on hyperspectral technology. In International Conference on Artificial Intelligence and Security, pp. 537-550. https://doi.org/10.1007/978-3-030-78621-2_45
[20] Mohite, J., Karale, Y., Pappula, S., TP, A.S., Sawant, S.D., Hingmire, S. (2017). Detection of pesticide (Cyantraniliprole) residue on grapes using hyperspectral sensing. In Sensing for Agriculture and Food Quality and Safety IX, pp. 192-199. https://doi.org/10.1117/12.2261797
[21] Tsuta, M., El Masry, G., Sugiyama, T., Fujita, K., Sugiyama, J. (2009). Comparison between linear discrimination analysis and support vector machine for detection of pesticide on spinach leaf by hyperspectral imaging with excitation-emission matrix. In ESANN'2009 proceedings European Symposium on Artificial Neural Networks - Advances in Computational Intelligence and Learning, Belgium, Bruges, pp. 337-342.
[22] Jiang, R., Zhuang, G., Xie, S., et al. (2025). Hyperspectral detection of pesticide residues in black vegetable based on multi-classifier entropy weight method. IEEE Access, 13: 55701-55711. https://doi.org/10.1109/ACCESS.2025.3553384
[23] He, H., Li, Z., Qin, Q., et al. (2025). Spectroscopic and imaging technologies combined with machine learning for intelligent perception of pesticide residues in fruits and vegetables. Foods, 14(15): 2679. https://doi.org/10.3390/foods14152679
[24] Chen, Z., Dong, X., Liu, C., Wang, S., Dong, S., Huang, Q. (2023). Rapid detection of residual chlorpyrifos and pyrimethanil on fruit surface by surface-enhanced Raman spectroscopy integrated with deep learning approach. Scientific Reports, 13(1): 19855. https://doi.org/10.1038/s41598-023-45954-y
[25] Basha, Z.S., Ram, B.G.S., Bama, B.S., Padmasri, P., Roomi, S.M.M. (2025). 3D-sersnet based pesticide residue detection in okra using hyperspectral imaging technology. Measurement: Food, 20: 100254. https://doi.org/10.1016/j.meafoo.2025.100254
[26] Jiang, R., Qu, D., Yin, R., Lu, S., Xie, S. (2025). Detection of pesticide residues in banana peel based on hyperspectral imaging and deep forest algorithms. In Proceedings of the 2025 International Symposium on Artificial Intelligence and Computational Social Sciences, pp. 245-252. https://doi.org/10.1145/3776759.3776797
[27] Phegade, S.G., Khachane, M.Y. (2024). SpinachHsiDB—A hyperspectral image dataset to detect pesticides sprayed leaves and fresh leaves. Journal of

Vytapeni, 12(11): 192-202.
[28] Yan, Y.J., Wong, W.K., Chen, C.J. et al. (2023). Hyperspectral signature-band extraction and learning: an example of sugar content prediction of Syzygium samarangense. Scientific Reports, 13: 15100. https://doi.org/10.1038/s41598-023-41603-6
[29] Batool, A., Byun, Y.C. (2023). Lightweight EfficientNetB3 model based on depthwise separable convolutions for enhancing classification of leukemia white blood cell images. IEEE Access, 11: 37203-37215. https://doi.org/10.1109/ACCESS.2023.3266511
[30] Tan, M., Le, Q.V. (2019). EfficientNet: Rethinking model scaling for convolutional neural networks. arXiv preprint arXiv:1905.11946. https://doi.org/10.48550/arXiv.1905.11946
[31] Selvaraju, R.R., Cogswell, M., Das, A., Vedantam, R., Parikh, D., Batra, D. (2020). Grad-CAM: Visual explanations from deep networks via gradient-based localization. International Journal of Computer Vision, 128(2): 336-359. https://doi.org/10.1007/s11263-019-01228-7
[32] Panchbhai, K.G., Lanjewar, M.G. (2025). Enhancement of tea leaf diseases identification using modified SOTA models. Neural Computing and Applications, 37(4): 2435-2453. https://doi.org/10.1007/s00521-024-10758-2